Modeling Residual Displacements of Concrete Bridge Columns under Earthquake Loads Using Fiber Elements

Won K. Lee, P.E., A.M.ASCE[1]; and Sarah L. Billington, M.ASCE[2]

Abstract: Nonlinear dynamic analysis with fiber-element models is now widely used to assess the seismic response of bridge structures. The ability of such models to accurately simulate response parameters for characterizing the postearthquake condition of bridges, namely residual displacements, is assessed by comparison of analyses of dynamically loaded reinforced concrete bridge columns to experimental data. The models are unable to capture residual displacements, and the cause of the inability to capture residual displacements is investigated through dynamic analysis of fiber-element and single-degree-of-freedom (SDOF) models. A certain type of pinching present in the numerical hysteretic response shape is found to lead to poor residual displacement simulation both in the SDOF models and in fiber-element models. When eliminating this pinching, improvements to residual displacement simulation are found. A modified concrete constitutive model representing damage accumulation from cyclic loading is implemented for the fiber-element analysis that incorporates changes to reloading behavior when moving from high tensile strain back to compression. Analysis using the modified concrete constitutive model leads to improvements in the ability of the fiber-element model to capture residual displacements.

DOI: 10.1061/(ASCE)BE.1943-5592.0000059

CE Database subject headings: Displacements; Earthquake loads; Concrete structures; Highway and road structures; Hysteresis; Columns.

Author keywords: Residual displacements; Earthquake loads; Concrete structures; Highway and road structures; Hysteresis; Fiber elements.

Introduction

In recent years, the earthquake engineering community has been focusing attention on performance-based design in order to predict and manage better the postearthquake functionality and condition of structures. Excessive direct and indirect monetary losses due to nonstructural damage and downtime that were sustained in recent earthquakes (e.g., Kobe 1995; Northridge 1995; Loma Prieta 1989) revealed that the philosophy of designing only for life safety (i.e., collapse prevention) was not sufficient in meeting the diverse needs of structure owners and of society as a whole. The goal of performance-based design is to incorporate a predefined level of postearthquake performance into the design of a structure such that the damage is kept to "acceptable" levels, with the definition of acceptable varying on the type and use of a structure.

The research presented here focuses on bridge structures and in particular bridge column supports. Bridges are a key component in the transportation network, which provides emergency services immediately following an earthquake. The uninterrupted function of the transportation network is crucial to maintaining normal societal function. Standard highway bridges in highly seismic regions such as California are typically designed such that plastic behavior will concentrate in the columns during earthquakes. The columns are expected to undergo large inelastic deformations under severe earthquakes, which can result in residual displacements. These residual displacements are an important measure of postearthquake functionality in bridges, and can determine whether or not a bridge remains usable following an earthquake. For example, following the Kobe earthquake, over 100 reinforced concrete columns with a residual drift ratio (displacement normalized by column height) of over 1.5% were demolished even though they did not collapse (Kawashima et al. 1998). Residual displacement can often occur in columns that undergo only moderate inelastic displacements, where there is yielding of longitudinal reinforcement but no spalling of concrete cover or buckling or fracture of reinforcement.

The foundation of performance-based design is the ability to predict accurately the actual performance and behavior of structures under earthquake loading using analytical tools and models. In the case of bridge structures in particular, but also for building structures, residual displacement prediction is key to benchmarking the performance of current systems and comparatively assessing innovative systems such as self-centering systems (e.g., Kwan and Billington 2003a,b; Sakai et al. 2005). While prediction of peak dynamic responses (e.g., peak accelerations and displacements) has been extensively studied, the study of residual displacements has received almost negligible attention in comparison. In particular, the study of residual displacements using fiber-element models, which are becoming popular for nonlinear dynamic analysis, has received little attention.

[1]Engineer, Forell/Elsesser Engineers, Inc., 160 Pine St., Suite 600, San Francisco, CA 94111 (corresponding author). E-mail: wonlee21@gmail.com

[2]Associate Professor, Dept. of Civil and Environmental Engineering, Stanford Univ., 473 Via Ortega, Stanford, CA 94305-4020. E-mail: billington@stanford.edu

Note. This manuscript was submitted on August 24, 2008; approved on July 3, 2009; published online on July 13, 2009. Discussion period open until October 1, 2010; separate discussions must be submitted for individual papers. This paper is part of the ***Journal of Bridge Engineering***, Vol. 15, No. 3, May 1, 2010. ©ASCE, ISSN 1084-0702/2010/3-240–249/$25.00.

J. Bridge Eng. 2010.15:240-249.

In this study, the ability to capture residual displacements using fiber-element models is assessed by modeling a column from a set of shaking table tests of conventional reinforced concrete and post-tensioned concrete bridge columns. Several factors affecting the ability of a fiber-element model to predict residual displacements well are evaluated here and a previously developed constitutive model is identified that provides improved residual displacement response prediction.

Related Research

While numerous studies have been devoted to performance prediction of reinforced concrete columns under cyclic and seismic loading, a limited number of studies have been performed specifically with regard to predicting postearthquake residual displacements. These studies include the work by Mahin and Bertero (1981); Macrae and Kawashima (1997); Kawashima et al. (1998); Borzi et al. (2001); Christopoulos et al. (2003); Pampanin et al. (2003); Ruiz-Garcia and Miranda (2005); and Yazgan and Dazio (2006). With the exception of Yazgan and Dazio (2006), all of these studies involved the use of simplified hysteretic models for analyzing single-degree-of-freedom (SDOF) or multi-degree-of-freedom (MDOF) structures under earthquake excitations. These studies provide a wealth of information regarding the effect of a number of parameters for various hysteretic models (e.g., strength and postyielding stiffness) on residual displacements. However, these models are not as well suited for predictive design because the hysteretic response would need to be known a priori.

Fiber-element models are intended for use for predictive design and analysis of bridge and building structures under seismic loads. However fiber-element models have been found incapable of capturing any significant residual displacement (Sakai and Mahin 2004; Sakai et al., 2005; Yazgan and Dazio 2006). For example, Sakai and Mahin (2004) subjected a fiber-element model of a reinforced concrete column to a suite of near-fault ground motions and found that the model sustained peak drifts of on average 5%, while ending with residual drifts of on average only 0.2%. Greater residual displacements should be expected than are predicted by the fiber-element models as shown in experiments (e.g., Sakai et al. 2005; Hachem et al. 2003) as well as built reinforced concrete columns following earthquakes (e.g., following the Kobe earthquake).

Simulation of Dynamic Reinforced Concrete Column Experiments

Background on Experiments

Simulations conducted in this study were of a column from shake table tests in a previous study by Sakai et al. (2005). The specimen was a single 406-mm-diameter circular reinforced concrete column with a longitudinal reinforcing ratio of 1.20% and a transverse volumetric reinforcing ratio of 0.76%. The specimen had design parameters that are typical of reinforced concrete highway bridges in California. Axial load in the column, representing dead load, was applied through the use of large rectangular concrete blocks attached to the top of the column. In this way, the P-delta effect of the dead load would be represented in the experiment. The axial load ratio of the column from the dead load was 7%. The measured fundamental period of the column was 0.77 s. The concrete had a nominal 28-day compressive strength of 32 MPa.

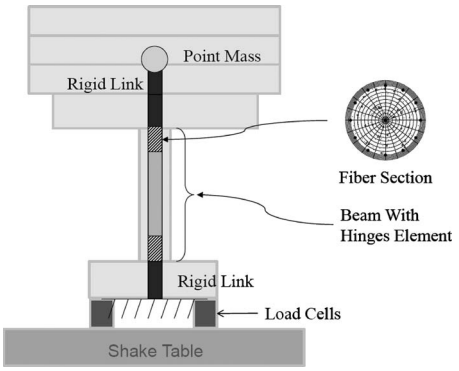

Fig. 1. Schematic of fiber-element model for RC column (adapted from Sakai 2005)

The column was tested on a bidirectional shaking table and was subjected to increasing levels of excitation using two orthogonal components (fault normal and fault parallel) of the Los Gatos record from the 1989 Loma Prieta Earthquake in California. In the experiment, the time values for the record were reduced by a factor of 2.12 to account for specimen scaling effects (Sakai et al. 2005). The column was first subjected to two low intensity inputs, corresponding to the record scaled to 7 and 10% of the as-recorded motion. The column was then subjected to a "design level" motion, with the motion scaled to 70%. The design level motion was intended to impose a displacement ductility demand in the specimen of roughly 4. Finally, the column was subjected to a "maximum level" motion, with the motion scaled to 100%. The maximum level motion was intended to impose a displacement ductility demand in the specimen of roughly 8. However, it was found after the experiment that the intended design level motion resulted in a displacement demand more representative of the desired maximum level demand. Therefore in this study, only the results from the motion scaled to 70% are used, as they are assumed to be representative of a maximum level event. Under this scaling level, no spalling of concrete and no buckling or fracture of reinforcement were observed.

Finite-Element Model

All analytical modeling performed herein was done using the OpenSees platform, (opensees.berkeley.edu). A schematic representation of the model used for the column is shown in Fig. 1. The column is modeled with a single force-based concentrated-plasticity (or lumped-plasticity) fiber element. The element is not a concentrated plasticity element in the conventional sense, wherein the nonlinear behavior is concentrated into moment-rotation springs at the ends of an element. Rather, the element is a fiber-based element with nonlinear constitutive behavior limited to specified plastic hinge regions at the ends of the element. The remainder of the element behaves linear elastically. Full details of the element formulation can be found in Scott and Fenves (2006).

The plastic hinge length for the column was calculated using the Caltrans Seismic Design Criteria (Caltrans 2001) equations for reinforced concrete columns. The elastic portion of the element is defined with three parameters: the elastic modulus and the moments of inertia in the two orthogonal bending directions. The elastic modulus used was that of the concrete, 560 MPa, computed using the ACI equation (ACI 2005) for normal weight concrete using the experimentally determined compressive strength.

J. Bridge Eng. 2010.15:240-249.

The effective moment of inertia was taken as 0.36 times the gross moment of inertia, and was computed using the Caltrans Seismic Design Criteria.

A three-dimensional model was created so that both components of the ground motion could be applied as in the experiment. The column is assumed fixed at the base. Both the confined and unconfined concrete are modeled using the stress-strain relationship described by the Kent-Scott-Park model (Scott et al. 1982) in compression and with no tensile strength. The use of a concrete constitutive model with no tensile strength is assumed to be appropriate for modeling of this column due to the fact that a number of lower intensity inputs were applied to the columns before the design and maximum level earthquakes were applied. These low level inputs were assumed to cause the concrete to crack but not to cause any other significant nonlinear behavior in the column. Both unloading and reloading follow the same linear path with a stiffness that is initially equal to the elastic modulus but that degrades with increasing strain according to Karsan and Jirsa (1969).

The fiber section used for the beam elements is discretized into core fibers (assumed to be confined by the spiral reinforcing) and cover fibers (unconfined). The unconfined compressive strength of the concrete was measured as 31.7 MPa, and this value is used to define the behavior of the cover concrete fibers. For the core concrete fibers, the peak compressive stress and strain are increased due to the confinement effect based on the Mander et al. (1983) model.

The stress-strain relationship for the bonded longitudinal reinforcing steel is described by the Giuffre-Menegotto-Pinto model (Taucer et al. 1991), which incorporates the Bauschinger effect for cyclic loading. For simplicity, bond slip in the reinforcing is not included in the model. Steel yield strengths were based on tensile tests of the reinforcing bars. A hardening ratio of 2% is assumed. A point mass is used to model the large rectangular concrete blocks above the column. Translational mass as well as rotational mass moments of inertia for a rectangular prism are defined for the point mass.

Among the limitations inherent in fiber-element models is the inability to capture local damage behavior such as fracture or buckling of longitudinal or transverse reinforcement. In the case of the column specimen and ground motion modeled here, none of the aforementioned damage was observed in the experiment.

Simulation Results

The column model was subjected to the Los Gatos motion scaled to 70%. Rayleigh damping with a damping ratio of 2% was applied. The value of 2% has been found to be applicable for reinforced concrete bridge structures (Hart and Vasudevan 1975). The simulated displacement response history in the fault normal direction of motion, recorded at the center of mass of the top blocks, is shown compared to the experimental response, also measured at the center of mass of the top blocks, in Fig. 2. The simulation predicts a peak displacement of 165 mm, while the experimental peak value was 155 mm (corresponding to a drift ratio of roughly 6.4%), a difference of approximately 6%. In the experiment, the column sustained a residual displacement of approximately 25 mm, corresponding to a drift ratio of slightly more than 1%. The simulation predicts a residual displacement of essentially zero.

Sensitivity studies were performed on several of the modeling parameters to determine their effect on the inability of the fiber-element model to capture any residual displacement. Among the parameters considered were the damping ratio, cracked moment of inertia, concrete tensile strength, concrete tension stiffening, and steel hardening ratio. While these analyses had an impact on peak displacements as expected, in no case did any of these sensitivity analyses result in capture of residual displacement.

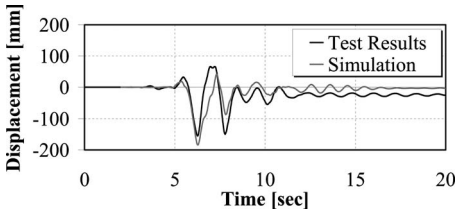

Fig. 2. Comparison of experimental and simulated displacement histories for RC column

The main conclusion from the modeling of the column by Sakai et al. (2005) is that although the simulation is able to capture the peak displacements for the column well, the residual displacement is not well predicted, and in fact no residual displacement is predicted at all. An investigation was performed to determine the cause of the inability to predict residual displacements in the model. In particular, the effect of ground motion and the impact of the shape of the hysteretic response on residual displacement simulation were studied.

Evaluation of Residual Displacement Prediction

Effect of Ground Motion

While the inability to predict residual displacements in the previous analysis is assumed to be due to the model, it is possible that the response was specific to the ground motion used. To rule out the possibility that it was a characteristic of the specific ground motion used that led to zero residual displacement in the analysis, the model was subjected to a suite of 20 additional unscaled near-fault ground motions (shown in Table 1). The ground motion set was taken from Somerville and Collins (2002). The fault-normal component of motion was used for all of the ground motions. Near-fault motions were selected as they were expected to provide a more severe response than far-field motions.

The resulting peak and residual displacements are plotted in Fig. 3 for the 20 earthquake ground motions. While several of the ground motions caused low responses in the column (e.g., Motions 13–17), a number of them caused significant peak displacements, with the largest peak displacement of approximately 360 mm resulting from ground Motion 7. While some of these values are very large and would likely lead to collapse in a physical column, the key observation is that in no case does the model retain any significant residual displacement. Such behavior would not be expected in an actual RC column. Although residual displacements will not always occur following an earthquake, it is unlikely that no residual displacements would occur in all of these cases. The results strengthen the assumption that it is the model that is unable to capture the residual displacements that would be expected in a physical system.

Fiber-Element Model Characteristics

One of the goals of performance-based engineering is to provide realistic assessments of the physical response of a structure during and following an earthquake; thus it is important that a model is

Table 1. Near-Fault Ground Motion Set

Number	Earthquake	Magnitude	Station	Distance (km)
1	Erzincan, Turkey	6.7	Erzincan	1.8
2	Kobe, Japan	6.9	Kobe JMA	0.5
3	Loma Prieta	7.0	Corralitos	3.4
4	Loma Prieta	7.0	Gavilan	9.5
5	Loma Prieta	7.0	Gilroy Historic	12.7
6	Loma Prieta	7.0	Lexington Dam	6.3
7	Loma Prieta	7.0	Los Gatos Pres. Center	3.5
8	Loma Prieta	7.0	Saratoga Aloha Ave.	8.3
9	Tottori, Japan	6.6	Kofu	10.0
10	Tottori, Japan	6.6	Hino	1.0
11	Coyote Lake	5.7	Coyote Lake Dam	4.0
12	Coyote Lake	5.7	Gilroy #6	1.2
13	Parkfield	6.0	Temblor	4.4
14	Parkfield	6.0	Array #5	3.7
15	Parkfield	6.0	Array #8	8.0
16	Livermore	5.5	Fagundes Ranch	4.1
17	Livermore	5.5	Morgan Territory Park	8.1
18	Morgan Hill	6.2	Coyote Lake Dam	0.1
19	Morgan Hill	6.2	Anderson Dam	4.5
20	Morgan Hill	6.2	Halls Valley	2.5

able to produce accurate predictions of residual displacements. While the accuracy of prediction of residual displacements under dynamic loading using analytical models has not received much attention, an improvement to the modeling approach used here is investigated in order to allow for at least some prediction of residual displacements. First, the hysteretic shape of the fiber-element model was studied. As a cyclic column test was not performed by Sakai et al. (2005), the cyclic response of the fiber-element model was compared to cyclic experimental data on a column of the same diameter and reinforcing ratio (i.e., 406.4 mm and 1.2%) tested by Hamilton et al. (2002). The column tested by Hamilton et al. (2002) had no axial load, and therefore for the sake of this comparison, the fiber-element model was analyzed with zero axial load.

The cyclic response of the fiber-element model of the column of Sakai et al. with no axial load is shown in Fig. 4(a). The experimental data from Hamilton et al. (2002) are shown in Fig. 4(b). The simulated and experimental load-displacement plots have similar behavior. Comparing the static residual displacements (displacement at zero load) after reaching a drift of 100 mm, the simulation predicts a value that is roughly 20% less than the value found in the experiment. The difference in the two can

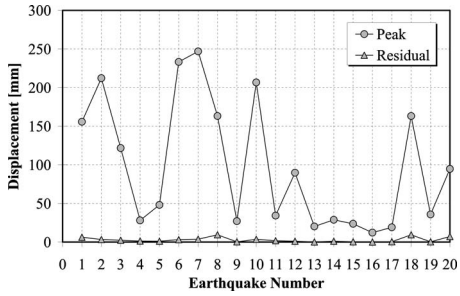

Fig. 3. Comparison of peak and residual displacements for fiber-element model subjected to near-fault ground motions

be found in the region from unloading in one direction to loading in the other direction. Consider first the final large cycle of the experimental response. The load-displacement plot traces out a smooth curve in moving from the positive to the negative loading direction. In contrast, this same portion of the curve in the fiber-element model response displays abrupt changes in stiffness and a flat region of near zero stiffness near the origin. This widely observed behavior can be seen as a sort of "pinching" in the hysteretic response and arises from the assumptions made in the constitutive models used, as will be discussed in following sections. Although the constitutive model for concrete used here was a model with no tensile strength, models including both tensile strength and tension stiffening effects yield similar hysteretic shapes (Lee 2007).

Impact of Hysteretic Response

To determine whether the inability of the dynamically loaded fiber-element model to capture residual displacements was due to its pinched hysteretic shape [Fig. 5(a)], a study was performed wherein SDOF models with two different hysteretic behaviors were subjected to earthquake motions and their residual displacements were monitored. First, a SDOF model was created with a hysteretic shape meant to emulate that of the fiber-element model. Next, a similar SDOF model was created, except with the pinching effect removed. These models are described as follows.

The model of Ibarra and Krawinkler (2005) was used as the base model for the SDOF hysteretic behavior. The envelope curve has an elastic region followed by a linear hardening region and a linear softening region. During unloading and reloading, the Ibarra and Krawinkler model dictates that the path will aim for the peak point after reaching zero force. Such behavior is not observed in the fiber-element model hysteresis, as the force continues past zero and into the opposite direction before flattening out and aiming for the peak point. To incorporate this behavior, the model was combined in parallel with an elastic-perfectly plastic model. To achieve the abrupt increase in stiffness near zero displacement, the model was again combined in parallel with a bilinear elastic model. The combined model displays the pinched effect as observed in the fiber-element model, and will herein be referred to as the PinchedSDOF model [Fig. 5(b)]. The PinchedSDOF model was created to have an initial stiffness equal to that of the fiber-element model. A second model, without pinching and referred to as the NoPinchingSDOF model, was created by combining the Ibarra and Krawinkler model with an perfectly elastic plastic model [Fig. 5(b)]. The initial stiffness of the NoPinchingSDOF model was the same as both the PinchedSDOF model and the original fiber-element model.

Two SDOF models, using the PinchedSDOF and NoPinchingSDOF hysteretic models, were then analyzed using the same suite of 20 earthquake records. The analyses were performed with viscous damping using a dashpot element with a damping ratio of 2%. The mass for the SDOF model was computed using the initial stiffness and period of the model, which were selected to match that of the fiber-element model. The peak and residual displacement responses for the SDOF models using the PinchedSDOF and NoPinchingSDOF hysteretic models are shown in Figs. 6 and 7, respectively. The results from the fiber-element analyses are shown in gray.

The results from the SDOF model with the PinchedSDOF hysteretic model are similar to the results of the fiber-element model. Such behavior was expected, as the PinchedSDOF model was created to mimic the behavior of the fiber-element model. The

J. Bridge Eng. 2010.15:240-249.

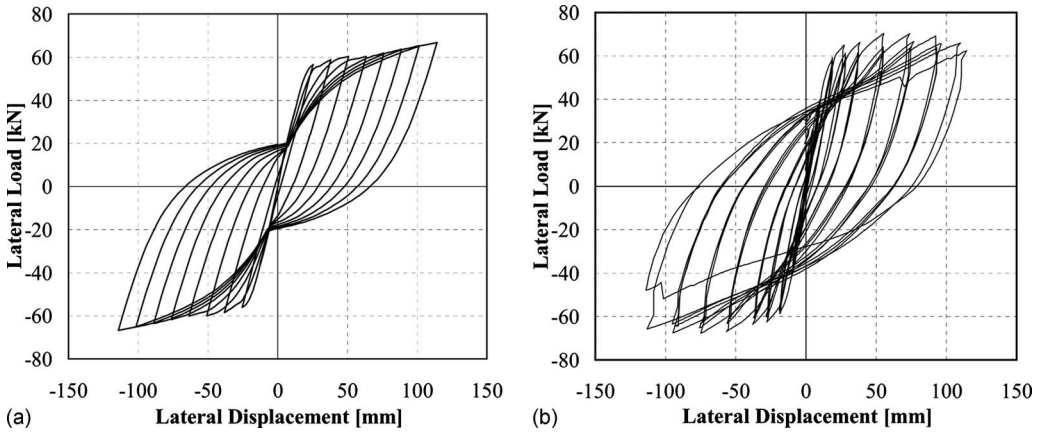

Fig. 4. Comparison of hysteretic response of (a) fiber-element model with no axial load; (b) experimental data (from Hamilton et al. 2002)

residual displacements were again essentially zero for all ground motions. The results from the SDOF model with the NoPinchingSDOF hysteretic model show similar peak displacements to the fiber-element model, but, in contrast to the NoPinchingSDOF model, show significant residual displacements for several of the ground motions (6 out of 20). The results of the analyses indicate that the pinched behavior of the fiber-element model does indeed affect the ability to capture residual displacements. When the hysteretic behavior is modified to remove this behavior, residual displacements can then be captured. While the accuracy of these values is unknown, the key observation is that the values are nonzero.

To understand why the hysteretic shape of the fiber-element model leads to very low residual displacements following dynamic loading, it is useful to examine more closely the results obtained from the SDOF analysis. Consider the response from record 20, which illustrates the effect well. The displacement time history and force-displacement response for the two models for this motion are shown in Fig. 8. For this ground motion, the peak displacement response of the two SDOF models are approximately equal, and also approximately equal to the value from the fiber-element model. However, the residual displacement value for the NoPinchingSDOF model is much larger than that of the PinchedSDOF model, which is almost zero.

The residual displacement can be seen to occur following the large pulse in the ground motion. The reason that the NoPinchingSDOF model retains a large residual displacement while the PinchedSDOF model does not is evident in the force-displacement response [Fig. 8(b)]. During the main pulse, the system is pushed to its maximum displacement of roughly 103 mm [shown with Arrow A in Fig. 8(a)]. The ground motion then gives the system a strong push in the opposite direction [shown with Arrow B in Fig. 8(a)]. In the case of the PinchedSDOF model, the model has almost zero stiffness during this push in the opposite direction (Path B), which allows the system to be pushed to near-zero displacement again. The system then reaches a jump in stiffness again near zero displacement, which tends to keep the system near zero displacement. In the case of the NoPinchingSDOF model, the system has stiffness during the push toward zero displacement (B to C), so it does not get pushed all the way back to near-zero displacement again [Point C in Fig. 8(b)]. For this reason, the NoPinchingSDOF model retains residual displacement while the PinchedSDOF model does not.

Selection of Concrete Constitutive Model to Capture Residual Displacements

Pinching in the hysteretic shape was identified in the SDOF analysis to inhibit the capture of residual displacements in dynamic analysis. Because this same pinching is present in the fiber-element model, modifications to the model were investigated to

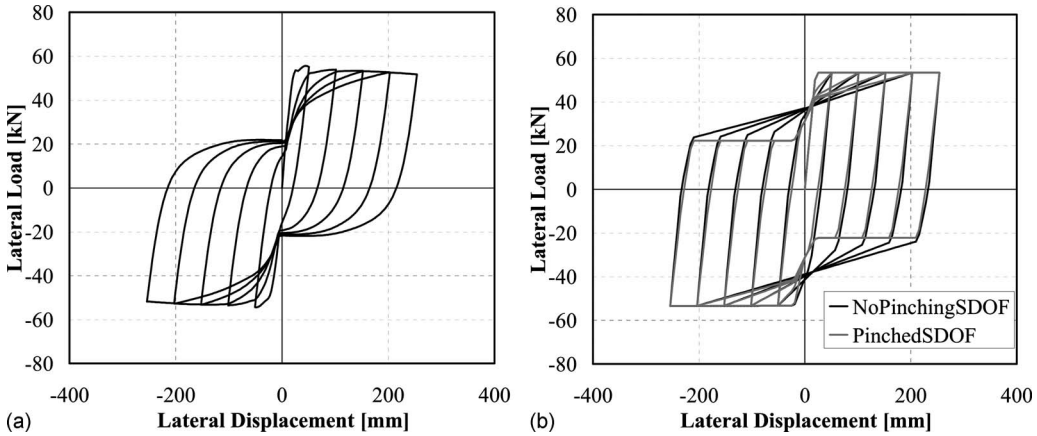

Fig. 5. Comparison of (a) fiber model hysteresis; (b) SDOF models

J. Bridge Eng. 2010.15:240-249.

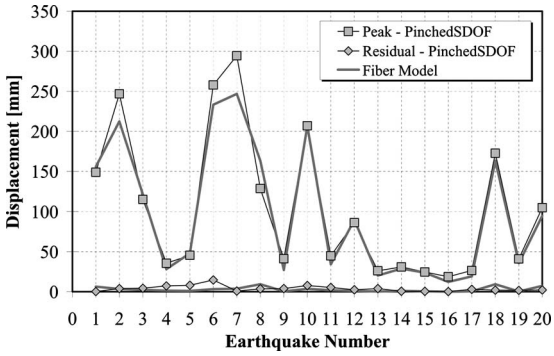

Fig. 6. Peak and residual displacement responses for PinchedSDOF model

determine how the pinching could be avoided and verify again that this would lead to improvements in the capture of residual displacements. It is noted that bond-slip behavior in reinforced concrete will lead to pinching in the hysteretic response. However for simplicity in modeling, bond-slip modeling was not evaluated here. Instead, modifications to the concrete constitutive model capturing the behavior that results from reinforcement slipping in concrete under cyclic load was investigated as discussed below.

To determine if the pinching in the model used here was caused by the concrete or the steel constitutive models, the stress-strain response of several concrete and steel fibers in the column fiber section was tracked with the load-displacement response of the column. The pinching in the fiber model with the constitutive models adopted here was found to result from the constitutive behavior of the concrete. Consider a concrete fiber on the left face of a column, whose behavior will be followed through part of the loading cycle of the column, as shown in Fig. 9. As the column is pushed to its maximum negative displacement [Region 1 in Fig. 9(a)], the concrete is somewhere on the envelope curve in compression [Region 1 in Fig. 9(b)]. As the column unloads [changes direction and begins to move in the positive direction, Region 2 in Fig. 9(a)], the concrete fiber unloads and quickly reaches zero stress [Region 2 in Fig. 9(b)]. As the column continues to move in the positive direction [Region 3 in Fig. 9(a)], the concrete fiber goes into tension, and still contributes no stiffness (at zero stress) to the column [Region 3 in Fig. 9(b)].

When the column reaches its maximum positive displacement, the column again changes direction and begins to unload [Region 4 in Fig. 9(a)]. During this portion, the concrete fiber reaches its maximum tensile strain and then begins to move back in the positive direction [Region 4 in Fig. 9(b)] along the zero stress axis and provides no stiffness to the column. At some point, the concrete fiber reaches the point of unloading, and begins to reload to the peak compressive strain [Region 5 in Fig. 9(b)]. It is at this stage where the concrete in compression again begins to contribute to the stiffness of the column. This point is easily identifiable in the load-displacement plot of the column where the stiffness abruptly increases [Region 5 in Fig. 9(a)]. As the column continues to load [Region 6 in Fig. 9(a)], the concrete again moves along the envelope curve [Region 6 in Fig. 9(b)].

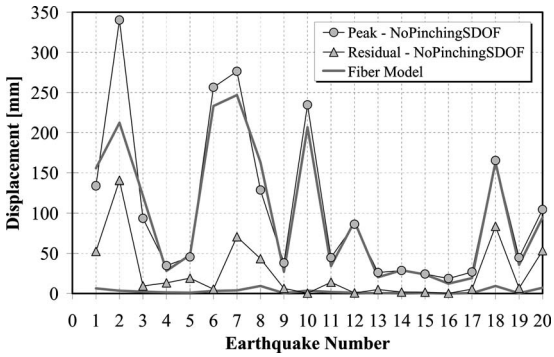

Fig. 7. Peak and residual displacement responses for NoPinching-SDOF model

The pinching effect in this model therefore arises from the reloading behavior of the concrete constitutive model from tension to compression. This type of reloading behavior is commonly used in cyclic concrete constitutive models. To smooth the unloading and reloading behavior of the fiber-element model's load-displacement behavior, the approach taken here was to modify the behavior of the concrete constitutive model when moving from tension back to compression. It was necessary for the model to be modified such that reloading could occur at a strain value [Point B in Fig. 10(b)] prior to that of the original unloading strain value [Point A in Figs. 9(a and b)].

The behavior represented by the modified model shown in Fig. 10(b) was observed in previous experimental research by Ma et al. (1976). It was observed that cracks in reinforced concrete members under cyclic loading can become partially filled with broken particles of hardened cement paste or aggregate (often the result of bond-slip, i.e., the movement of the reinforcement relative to the concrete), allowing load to be transferred across the crack before it has closed fully. Additionally, it is probable that when large cracks open and then close again, they will not align exactly as they did in the unfractured material, providing another mechanism for the transfer of stresses before the crack fully closes. Stanton and McNiven (1979) identified this issue and developed a constitutive model for concrete that incorporated this behavior.

A constitutive model for concrete incorporating the effect of aggregate trapped in cracks based on the Stanton and McNiven model was used for this research for the purpose of reducing the pinching observed in the fiber-element models, with the goal of allowing for improved capture of residual displacements. The model is essentially the same as the original model, i.e., the Kent-Scott-Park model in compression with no tension strength, and with unloading assumed to occur linearly according to the Karsan and Jirsa (1969) model. The modification is in the reloading from large tensile strains to compression.

The reloading behavior was kept as simple as possible with the goal of providing only necessary modifications to the hysteretic shape of the fiber-element model. In the modified model, the concrete reloads at a strain prior to the previous unloading strain. The model is peak oriented, similarly to the original concrete model, i.e., the stress path during reloading will aim toward the peak point (maximum compressive strain reached) on the envelope curve.

Unlike the Stanton and McNiven model (Stanton and McNiven 1979), the model used here assumes the reloading strain value to be a constant for simplicity. This strain value at which reloading is assumed to occur [Point B in Fig. 10(b)], defined now as the reloading strain (ε_r), is assumed to be a positive (tensile) value and is an additional parameter that must be specified to the model. Because the reloading strain is set at a constant positive value, the model will function in exactly the same manner as the original concrete model if this value is not exceeded, i.e., if the concrete does not go too far into tension. Only if the strain ex-

J. Bridge Eng. 2010.15:240-249.

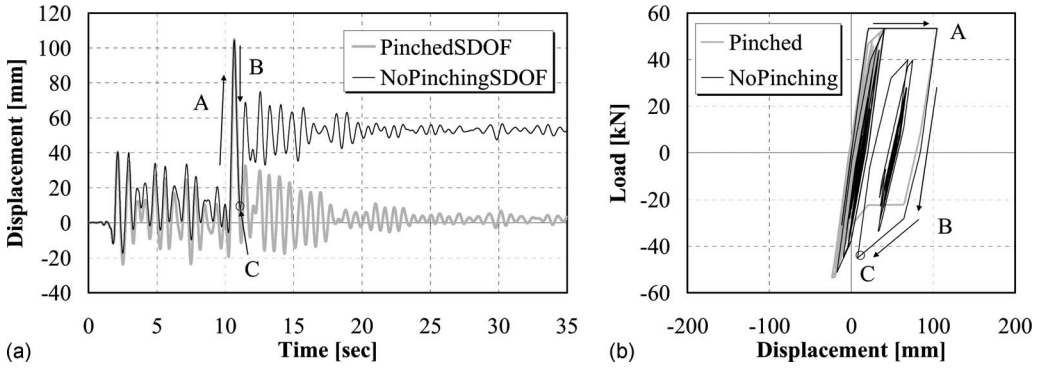

Fig. 8. Comparison of (a) displacement time history; (b) force-displacement response for SDOF models under earthquake Motion 20

ceeds this value will the alternate reloading be "activated" and the model will become different from the original concrete model. The physical reasoning for this is that cracks are assumed to have to reach a certain size before particles can become trapped in them. Therefore ε_r has a physical correlation to crack width opening.

In the model used here, if unloading occurs while on the alternate loading path, it is assumed to occur along the same path for simplicity. In reality, the unloading would be expected to occur more quickly, i.e., along a steeper path as in the model of McNiven and Stanton (1979). However, the simplification assumed here is not expected to affect significantly the overall behavior of the column. Full details of the implementation of the model can be found in Lee (2007).

Analysis of RC Column with Modified Concrete Constitutive Model

The original fiber-element model for the RC column tested by Sakai et al. (2005) was reanalyzed using the modified concrete model with various values of the reloading strain value, ε_r. The modified model was used for the core fibers only, while the cover fibers were modeled with the unconfined concrete model. The results from a cyclic analysis are shown in Fig. 11, along with the behavior of the original model using the original concrete model.

It can be seen that depending on the value of ε_r that is used, the level of pinching that occurs in the fiber-element model can be reduced to varying degrees. For a value of ε_r=0.02, the abrupt stiffness change at around zero displacement for the fiber-element model is smoothed out to some degree. Although this change is subtle, its effect on the residual displacement response of the fiber element is in fact quite substantial. The fiber-element model using the modified concrete model was again analyzed under the suite of 20 ground motions and the peak and residual displacement responses were monitored. The results of these analyses are shown in Fig. 12.

The peak displacements predicted by the modified concrete model are all essentially the same as those predicted by the unmodified model. The results show that the use of the modified constitutive model can allow for some prediction of residual displacements. It can be seen that for several of the ground motion records, there are residual displacements where none were predicted using the original concrete model. Furthermore, many of these residual displacement values are not negligible and even arise after what might not be considered as excessive peak displacements. For example, Ground Motion 20 causes a peak displacement of 95 mm (a drift ratio of approximately 3.9%), and results in a residual displacement of 29 mm (a drift of roughly 1.2%). This residual displacement value would likely be considered as leaving the structure in or near an unusable state.

The results shown in Fig. 12 also indicate that the magnitude of the residual displacement does not necessarily correlate to the peak displacement reached. For example, Ground Motion 1 has a peak displacement 1.4 times greater than Ground Motion 2, but a residual displacement 5.2 times smaller. While large peak dis-

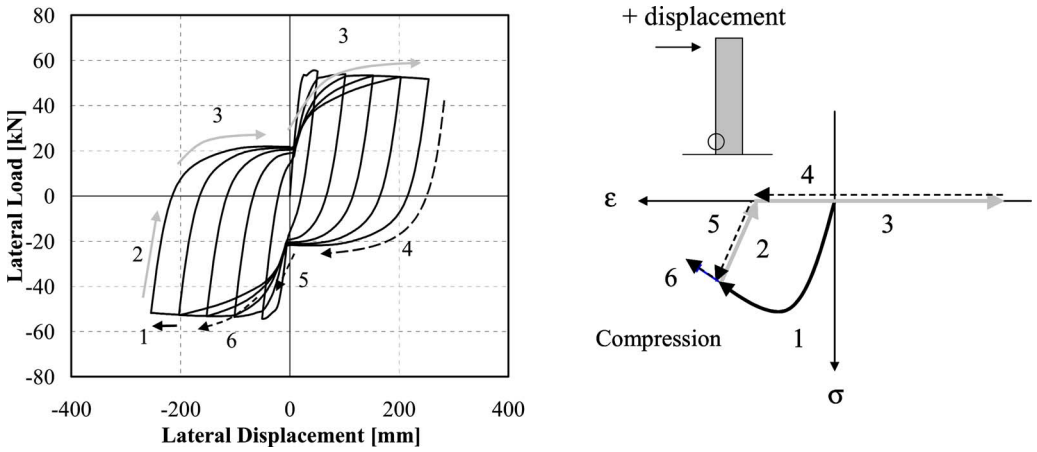

Fig. 9. Effect on (a) fiber-element model hysteresis from (b) constitutive behavior of concrete

J. Bridge Eng. 2010.15:240-249.

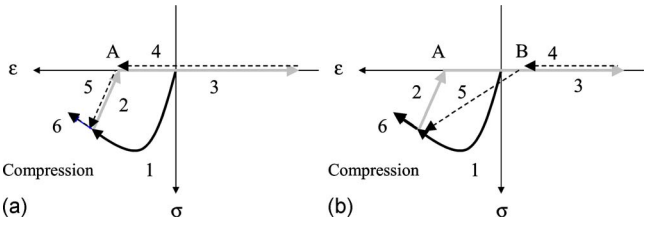

Fig. 10. Constitutive behavior of concrete in (a) unmodified; (b) modified model during unloading and reloading

placements may often be accompanied by large residual displacements, it would appear that in general the magnitude of residual displacements may not necessarily be predicted well by the magnitude of the peak displacements, and warrants further detailed study.

The fiber-element model with the modified concrete model using a value of $\varepsilon_r = 0.02$ was compared against the experimental response of the RC column tested by Sakai et al. (2005). The response of the model with the modified model is compared to both the experimental response and the response with the unmodified concrete model in Fig. 13. The response using the modified concrete model results in the same peak displacement as with the original concrete model, but clearly provides an improved simulation of residual displacement, where none was captured before.

The model with the same value of $\varepsilon_r = 0.02$ was then compared against another shaking table test of a circular RC column performed by Hachem et al. (2003). In this test, an RC column specimen identical to that of the RC column tested by Sakai et al. (2005) was tested on a shaking table and subjected to the Olive View record from the 1994 Northridge earthquake. Hachem et al. (2003) modified the record by scaling the accelerations by a factor of 1.09 and reducing the time by a factor of 2.12 to account for specimen scaling effects. A comparison of the displacement response history for the experimental results and fiber-element models using the modified and unmodified models is shown in Fig. 14. Again, using the modified concrete model results in the same peak displacement as the unmodified model, but provides better capture of the residual displacement. While the modified concrete model allows the fiber-element model to capture residual displacements, the value of ε_r used to define the model is not based on theory and should be more properly calibrated to further experimental data in the future.

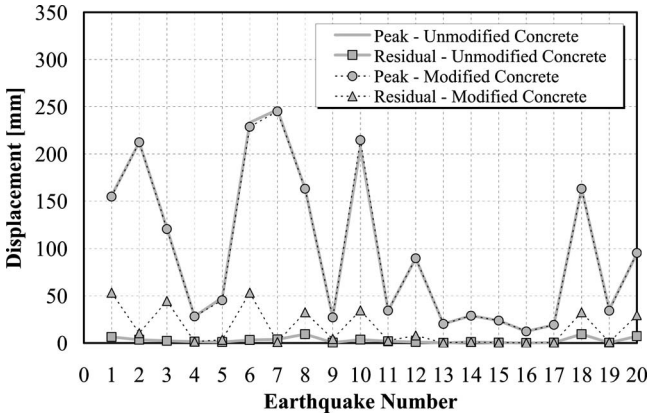

Fig. 12. Comparison of peak and residual displacement responses for fiber-element model with modified and unmodified models

Two problems arise regarding the calibration of the ε_r parameter at this time. The first is that the value is a parameter defining the constitutive behavior of the concrete, but may also depend on other factors relating to the member (such as geometry and reinforcing ratio). The second is the question of how this value should be calibrated. Calibration could be performed by matching the residual displacements of a simulated cyclic response to those of quasi-static, cyclic testing data or calibration could be performed by matching the residual displacements of dynamic testing data. A comparison of the columns of Sakai et al. (2005) and Hamilton et al. (2002) showed that matching residual displacements of quasi-static, cyclic data may not be adequate for predicting residual displacements under dynamic loading (Fig. 4). Calibration to dynamic testing data would likely be the best approach. However to date there is a lack of large numbers of tests.

It is also recognized that the pinched behavior in the hysteretic shape of the fiber-element model could be modified in other ways different than the approach used by the writers, i.e., there may be methods for smoothing the pinched hysteretic response other than the use of the modified concrete constitutive model. Alternatively, the model here could be combined with elements that capture additional mechanisms that contribute to pinching such as strain penetration (Zhao and Sritharan 2007). The key conclusion drawn from this study is that the pinched response in the hysteretic shape, in general and specifically for the fiber-element model, does affect the ability to capture residual displacements. Again, it

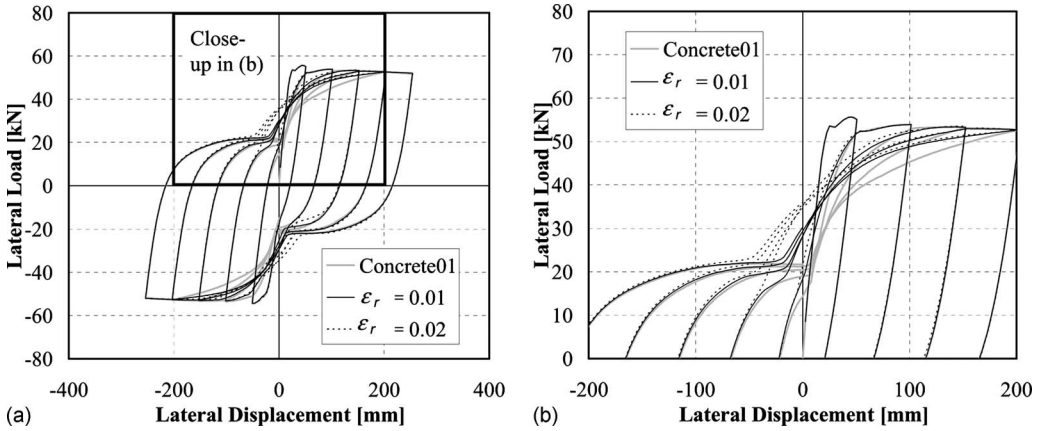

Fig. 11. (a) Load-displacement behavior of fiber-element model; (b) closeup view of SITC effect on hysteresis behavior

J. Bridge Eng. 2010.15:240-249.

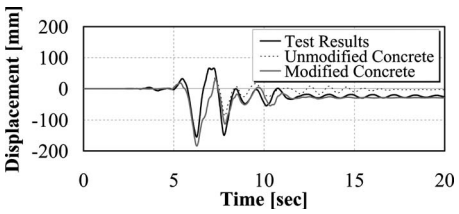

Fig. 13. Experimental and simulated displacement response histories using modified concrete model for RC column

is noted that the residual displacements discussed here are those that occur in columns that undergo some inelasticity, but not severe damage such as buckling or fracture of reinforcing bars. It is these residual displacements that are poorly captured by the artificial pinched response in the hysteretic shape, rather than those caused by severe levels of damage (buckling or fracture of reinforcing bars).

Conclusions

The prediction of peak and residual displacements is key to assessing the seismic performance of reinforced concrete members in the context of performance-based earthquake engineering. The ability to simulate the dynamic behavior, primarily with respect to residual displacements, of reinforced concrete bridge columns using fiber-element models is assessed here by comparison to experimental data. The following conclusions can be drawn:

- Dynamic analysis of SDOF models revealed that a certain type of pinching in the hysteretic behavior leads to an inability to capture residual displacements. Removal of the pinching allowed for improved residual displacement capture in the SDOF models. This type of pinching also exists in the fiber-element model used in this study;
- Dynamic, time-history analysis results indicated that the poor ability to capture residual displacement was due to attributes of the fiber-element model's hysteretic response rather than a specific characteristic of a ground motion;
- The constitutive model for concrete used in the fiber-element models, which is representative of commonly used concrete constitutive models, causes pinching in the hysteretic response that is not observed in experimental responses. The cause of the pinching stems from the reloading behavior of the constitutive model when moving from high tensile strains back to compression;
- Analysis of the fiber-element model using a modified version of the Stanton and McNiven concrete constitutive model to reduce pinching led to improvements in the ability of the fiber-element model to capture residual displacements; and
- One of the parameters used in the modified constitutive model has not been extensively calibrated to experimental testing data due to the lack of availability of a large database of easily-accessible, existing data. Further calibration should be performed with available existing data.

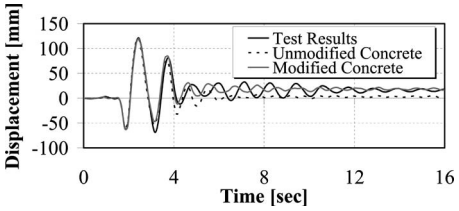

Fig. 14. Experimental and simulated displacement response histories using modified concrete model in the fault normal direction for RC column subjected to Olive view record

Acknowledgments

This research was sponsored by the Earthquake Engineering Research Centers Program of the National Science Foundation through the Pacific Earthquake Engineering Research Center. The opinions expressed in this paper are those of the writers and not necessarily of the sponsor. Enlightening discussions with Professor John Stanton of the University of Washington regarding constitutive modeling of concrete and the SITC effect are gratefully acknowledged. Experimental data from Dr. Junichi Sakai and Dr. Mahmoud Hachem from their work at the University of California, Berkeley, are also greatly appreciated.

Notation

The following symbols are used in this paper:

f_{pu} = ultimate strength of prestressing steel; and

ε_r = reloading strain value for concrete constitutive model.

References

American Concrete Institute (ACI). (2005). "Building code requirements for structural concrete and commentary." *ACI 318–05*, American Concrete Institute, Farmington Hills, Mich.

Borzi, B., Calvi, G. M., Elnashai, A. S., Faccioli, E., and Bommer, J. J. (2001). "Inelastic spectra for displacement-based seismic design." *Soil. Dyn. Earthquake Eng.*, 21(1), 47–61.

Caltrans. (2001). *Seismic design criteria V. 1.2*, Caltrans, Sacramento, Calif.

Christopoulos, C., Pampanin, S., and Priestley, M. N. (2003). "Performance-based seismic response of frame structures including residual deformations. Part I: Single-degree of freedom systems." *J. Earthquake Eng.*, 7(1), 97–118.

Hachem, M. M., Mahin, S. A., and Moehle, J. P. (2003). "Performance of circular reinforced concrete bridge columns under bidirectional earthquake loading." *Rep. No. PEER 2003/06*, Pacific Earthquake Engineering Research Center, Univ. of California, Berkeley, Calif.

Hamilton, C. H., Pardoen, G. C., and Kazanjy, R. P. (2002). "Experimental testing of bridge columns subjected to reversed-cyclic and pulse-type loading histories." *Rep. No. 2001-03*, Civil Engineering Technical Report Series, Univ. of California, Irvine, Calif.

Hart, G. C., and Vasudevan, R. (1975). "Earthquake design of buildings: Damping." *J. Struct. Div.*, 101(1), 11–30.

Ibarra, L. F., and Krawinkler, H. (2005). "Global collapse of frame structures under seismic excitations." *Blume Center Technical Rep. No. 152*, John A. Blume Earthquake Engineering Center, Stanford Univ., Stanford, Calif.

Karsan, I. D., and Jirsa, J. O. (1969). "Behavior of concrete under compressive loadings." *J. Struct. Div.*, 95(12), 2543–2563.

Kawashima, K., MacRae, G., Hoshikuma, J., and Nagaya, K. (1998). "Residual displacement response spectrum." *J. Struct. Eng.*, 124(5), 523–530.

Kwan, W., and Billington, S. (2003a). "Unbonded posttensioned concrete bridge piers. I: Monotonic and cyclic analyses." *J. Bridge Eng.*, 8(2), 92–101.

Kwan, W., and Billington, S. (2003b). "Unbonded posttensioned concrete

bridge piers. II: Seismic analyses." *J. Bridge Eng.*, 8(2), 102–111.
Lee, W. K. (2007). "Simulation and performance-based earthquake engineering assessment of self-centering, posttensioned concrete bridge systems." Ph.D. dissertation, Stanford Univ., Stanford, Calif.
Ma, S., Bertero, V., and Popov, E. (1976). "Experimental and analytical studies on the hysteretic behavior of reinforced concrete rectangular and T-Beams." *Rep. No. EERC 76-2*, Earthquake Engineering Research Center, Univ. of California, Berkeley, Calif.
Macrae, G., and Kawashima, K. (1997). "Post-earthquake residual displacements of bilinear oscillators." *Earthquake Eng. Struct. Dyn.*, 26, 701–716.
Mahin, S., and Bertero, V. V. (1981). "An evaluation of inelastic seismic design spectra." *J. Struct. Eng.*, 107(ST9), 1777–1795.
Mander, J., Priestley, M. N., and Park, R. (1983). "Seismic design of bridge piers." *Rep. No. 84-02*, Univ. of Canterbury, Christchurch, New Zealand.
Pampanin, S., Christopoulos, C., and Priestley, M. N. (2003). "Performance-based seismic response of frame structures including residual deformations. Part II: Multi-degree of freedom systems." *J. Earthquake Eng.*, 7(1), 119–147.
Ruiz-Garcia, J., and Miranda, E. (2005). "Performance-Based assessment of existing structures accounting for residual displacements." *Blume Center Technical Rep. No. 153*, John A. Blume Earthquake Engineering Center, Stanford Univ., Stanford, Calif.
Sakai, J. (2005). "Single reinforced concrete bridge column (Specimen B)." ⟨http://library.eerc.berkeley.edu/archives/sakai/exp/specB.html⟩.
Sakai, J., Jeong, H., and Mahin, S. (2005). "Earthquake simulator tests on the mitigation of residual displacements of reinforced concrete bridge columns." *Proc., 21st U.S.-Japan Bridge Engineering Workshop*, Tsukuba, Japan.
Sakai, J., and Mahin, S. (2004). "Mitigation of residual displacements of circular reinforced concrete bridge columns." *Proc., 13th World Conf. on Earthquake Engineering*, Vancouver, Canada.
Scott, B., Park, R., and Priestley, M. N. (1982). "Stress-strain behavior of concrete confined by overlapping hoops at low and high strain rates." *J. Am. Concr. Inst.*, 79(1), 13–27.
Scott, M., and Fenves, G. (2006). "Plastic hinge integration methods for force-based beam-column elements." *J. Struct. Eng.*, 132(2), 244–252.
Somerville, P., and Collins, N. (2002). "Ground motion time histories for the I880 Bridge–Oakland." *PEER Technical Rep. Prepared for Pacific Earthquake Engineering Research Center*, Univ. of California, Berkeley, Calif.
Stanton, J., and McNiven, H. (1979). "The development of a mathematical model to predict the flexural response of reinforced concrete beams to cyclic loads, using system identification." *Rep. No. EERC 79-02*, Earthquake Engineering Research Center, Univ. of California, Berkeley, Calif.
Taucer, F., Spacone, E., and Filippou, F. (1991). "A fiber beam-column element for seismic response analysis of reinforced concrete structures." *UCB/EERC Technical Rep. No. 91/17*, Earthquake Engineering Research Center, Univ. of California, Berkeley, Calif.
Yazgan, U., and Dazio, A. (2006). "Comparison of different finite-element modeling approaches in terms of estimating the residual displacements of rc structures." *Proc., 8th U.S. National Conf. on Earthquake Engineering*, San Francisco.
Zhao, J., and Sritharan, S. (2007). "Modeling of strain penetration effects in fiber-based analysis of reinforced concrete structures." *ACI Struct. J.*, 104(2), 133–141.

J. Bridge Eng. 2010.15:240-249.